nature plants

SUPPLEMENTARY INFORMATION

DOI: 10.1038/NPLANTS.2015.160

Woody biomass production lags stem-girth increase by over one month in coniferous forests

Henri E. Cuny, Cyrille B.K. Rathgeber, David Frank, Patrick Fonti, Harri Mäkinen, Peter Prislan, Sergio Rossi, Edurne Martinez del Castillo, Filipe Campelo, Hanuš Vavrčík, Jesus Julio Camarero, Marina V. Bryukhanova, Tuula Jyske, Jožica Gričar, Vladimír Gryc, Martin De Luis, Joana Vieira, Katarina Čufar, Alexander V. Kirdyanov, Walter Oberhuber, Vaclav Treml, Jian-Guo Huang, Xiaoxia Li, Irene Swidrak, Annie Deslauriers, Eryuan Liang, Pekka Nöjd, Andreas Gruber, Cristina Nabais, Hubert Morin, Cornelia Krause, Gregory King & Meriem Fournier.

DOI: 10.1038/NPLANTS.2015.160

Supplementary Methods

Study sites for detailed monitoring of wood formation

Three intensively studied sites were selected in mixed mature temperate forests composed of silver firs (*Abies alba* Mill.), Norway spruces (*Picea abies* [L.] Karst.) and Scots pines (*Pinus sylvestris* L.) in the Vosges Mountains (northeast France). The three sites were spread on a north-south axis of about 15 km and were named according to the closest town: Walscheid (370 m ASL, 48°38'N, 7°09'E), Abreschviller (430 m ASL, 48°36'N, 7°08'E) and Grandfontaine (650 m ASL, 48°28'N, 7°08'E). On each site, pits were dug to depict soil profiles, and complete inventories were built to describe stand structure. Based on these inventories, five dominant and healthy trees of silvers fir, Norway spruce and Scots pine were selected on each site, for a total of 45 studied trees (5 trees × 3 species × 3 sites) for 3 years (2007–2009) of wood formation monitoring (Supplementary Table 2).

Dendrometer and meteorological data

Manual band dendrometers (DB-20, EMS Brno, Czech Republic) were installed at breast height in March 2007 on the stem of all selected trees, after the removal of most part of the dead bark, and were read weekly thereafter to monitor stem circumference variations. Changes in stem girth measured by band dendrometers were transformed into stem radial variations assuming a circular cross section of the stem.

Daily meteorological data (temperature, precipitation, cumulative global radiation, wind speed, and relative air humidity) of the monitoring period were gathered from three meteorological stations, each of them located less than 2 km from the corresponding site.

Modelling soil water balance and characterising the seasonality of environmental factors

We used the model Biljou© to assess the daily water balance of the three studied stands during the three monitoring years (https://appgeodb.nancy.inra.fr/biljou/)[1]. In addition to the daily meteorological data mentioned above, the model takes as input soil (*e.g.*, number and depth of layers, and proportion of fine roots per layer), and stand (forest type and maximum leaf area index) parameters, and gives as output the relative extractable water (REW) on a daily scale. The REW is a relative expression of the filling state of the soil: REW is 100% at field capacity, and 0% at the permanent wilting point. Water stress is assumed to occur when the REW drops below a threshold of 40%, under which transpiration gradually decreases due to stomata closure[1].

Daily water balance and meteorological data (temperature and light radiation) were smoothed using generalised additive models (GAMs) in order to obtain representative seasonal trends of climatic conditions[2]. GAMs were fitted in R[3] using the mgcv package[4].

Xylem collection, preparation and observation

To monitor tree-ring formation of each selected tree, small wood samples (2 mm thick and 1.5 cm long microcores including the phloem, cambial zone, the forming ring and some previous rings) were collected weekly on tree stem, from April to November during three years (2007–2009), for a total of about 32 microcores per tree and per year. Microcores were collected at breast height on the stems of the selected trees using a Trephor® (Vitzani, Belluno, Italy)[5]. The injury by a 1.5–2.5 mm diameter corer stimulates growth for about 2 mm on each side of the wound and for about 1 cm above and below[6]. Thus, for each tree the orientation on the stem of the first sampling was randomly selected among the four cardinal points, and successive microcores were then taken about 1 cm apart from each other and following a slightly ascending spiral pattern (about 30 cm in height between the first and the last sample of the year)[7] to avoid wound reaction without considerably increasing the

DOI: 10.1038/NPLANTS.2015.160

influence of stem circumferential variability on the final dataset.

Microcores were prepared in the laboratory, and transverse sections with 5–10 µm in thickness were cut with a rotary microtome (HM 355S, MM France). Sections were stained with cresyl violet acetate and permanently mounted on glass slides using Histolaque LMR®. Overall, about 4,300 anatomical sections were analysed using an optical microscope (AxioImager.M2, Carl Zeiss SAS, France) to track tree-ring formation. Sections were observed under visible and polarised light, at ×100–400 magnification. Resin ducts are anatomical features normally produced in Scots pine and Norway spruce wood, whereas they only appear in response to wounding in silver fir. However, for the three species, resin ducts were scarce on the sections, so that the anatomical observations and cell counting were always performed on tracheid radial files having no resin ducts.

We distinguished and counted the cambial, enlarging, wall thickening and mature cells along at least three radial files of the forming tree ring. Cells of the cambial zone divide by mitosis to produce xylem cells on the pith side, and phloem cells on the bark side. They had rectangular shape, thin primary walls and small radial diameters, around 5–8 µm. Once produced, xylem cells enter the enlargement phase, where they undergo marked radial diameter increase under turgor pressure and deposition of primary wall material[8]. Therefore, we described enlarging cells as being at least two times larger than cambial cells, but still surrounded by thin walls. After enlargement, cells undergo secondary wall formation and lignification (of both primary and secondary walls). The formation of the multi-layered secondary wall starts with the deposition of cellulose and hemicellulose microfibrils[9], while lignin is deposited afterwards in the remaining spaces to cement the microfibrils together[10]. Because secondary wall formation and lignification processes largely overlap, they were not discriminated and regrouped under the term “wall thickening”. We distinguished thickening cells thanks to the birefringence of the secondary walls — cellulose microfibrils are deposited

according to a particular orientation in the secondary wall that makes them shining under polarised light[11]. Furthermore, cresyl violet acetate staining, whereby cellulose is stained purple and lignin blue[12], was used to follow the advancement of lignification. So, thickening cells exhibited violet and blue walls, indicating that lignification was in progress, whereas mature tracheids exhibited plain blue walls, indicating that lignification was over. To reduce the noise due to eccentric growth in the dataset, current cell counts were standardised by previous year cell number[13], using the R package CAVIAR[3,14].

Characterisation of wood formation dynamics

In order to characterise intra-annual wood formation dynamics, we fitted generalised additive models (GAMs) on the standardised number of cells counted weekly in the cambial, enlargement, wall thickening, and mature zones of xylem differentiation[2]. Thanks to their flexibility, GAMs have proved to be particularly well-suitable to model the complex intra-annual patterns that characterise wood formation dynamics[2], and thus to accurately quantify the kinetics of xylem cell development[15].

GAMs are semi-parametric extensions of GLMs, which are themselves mathematical extensions of linear models[4,16]. Let us consider the linear model which has the form:

$$Y = \alpha + X\beta + \varepsilon \qquad (1)$$

where Y denotes the response variable, α is a constant called the intercept, $X = (X1, \ldots Xp)$ is the matrix of p predictor variables, $\beta = (\beta 1, \ldots, \beta p)$ is the vector of p regression coefficients (one for each predictor), and ε is the error term. Two main assumptions limit the use of this linear model: (a) the errors are assumed to follow a normal (Gaussian) distribution and to have a constant variance; (b) the predictors are assumed to have a linear effect on the response variable. By applying a mathematical transformation to the response variable Y according to the real distribution of the errors, GLMs relax these assumptions and thus generalise the linear

DOI: 10.1038/NPLANTS.2015.160

model to non-linear responses (but the linearity of components contributing to the predictor is preserved) and variables that can have other than a normal distribution (hence the name Generalised Linear Models), including the normal, binomial, Poisson, or gamma probability distributions[17,18]. The mathematical function used to transform the response variable is called the "link function" because it provides the relationship between the linear predictor (Xβ) and the expected value of the response variable Y, so that a GLM takes the form:

$$g(E(Y)) = \alpha + X\beta + \varepsilon \quad (2)$$

where g() is the link function, E(Y) is the expected value of Y and α, X, and β are those previously described in Eq. (1). The link function depends on the distribution of the response variable (and so of its error). In this study, the response variable corresponds to the number of cells weekly counted in the wood formation phases. Count data followed a Poisson distribution, and in this case the link function used is the log function (the model is a log-linear model). Note that if the variable follows a normal distribution with a constant variance, the link function is the identity function g(E(Y))) = Y, so that we obtained the classical linear model we saw in Eq. (1), which can be considered as a special case of GLMs.

A GAM is a GLM in which the linear predictor depends, in part, on a sum of smooth functions of predictors[4]. As for GLMs, the probability distribution of the response variable must still be specified. Therefore, GAMs are a semi-parametric generalisation of GLMs, and they take the form:

$$g\big(E(Y)\big) = \alpha + X\beta + \sum s_j(X_j) + \varepsilon \quad (3)$$

where X = (X1, …, Xp) is a matrix for any strictly parametric model components with parameter vector β, $s_j()$ are unspecified smooth functions for the covariates X_j, and g(), E(Y) and α are those previously described in Eq. (1) and (2).

The strength of GAMs lies in their flexibility, *i.e.* their ability to deal with non-linear and non-monotonic relationships between the response and the set of explanatory variables.

This is because the data determine the nature of the relationship between the response and the set of explanatory variables rather than assuming some form of parametric relationship[16,19]. GAMs are thus referred to as being data driven rather than model driven, because the data determine the nature of the relationship between the response variable and the set of explanatory variables rather than assuming a certain type of parametric relationship[16]. Because of their flexibility, GAMs have proved to be particularly well-suitable to model the complex intra-annual patterns that characterise wood formation dynamics[2], and thus to accurately quantify the kinetics of xylem cell development[15].

In the case of wood formation dynamics, we want to express the response variables, corresponding to the number of cells weekly counted in the wood formation phases, as a function of the day of year. Thus, the expression of our GAM simply began:

$$log\big(E(N)\big) = \alpha + s(DY) + \varepsilon \qquad (4)$$

where N is the vector of the number of cells weekly counted in the considered phase, and DY is the vector of the corresponding days of year.

GAMs were fitted in R[3] using the mgcv package[4] for every year on each individual tree. The values of the fitted models were then averaged to calculate means representing the general wood formation dynamics by species, site, and year.

For each mean series, the daily rate of xylem cell production-was calculated as the difference between the total numbers of cells predicted by GAMs on the consecutive days. Moreover, we used the average cell numbers predicted by GAMs to calculate the date of entrance of each cell in each development zone (cambial, enlargement, wall thickening and mature zones)[2]. From these dates, the durations spent by each cell in the enlargement and wall thickening zone were computed. The rates of radial diameter enlargement and wall deposition were computed for each cell by dividing its final dimensions (cell radial diameter and wall

DOI: 10.1038/NPLANTS.2015.160

cross area) – measured from image analysis of the entirely formed tree ring at the end of the season[15] – by the duration spent in the corresponding phase.

Calculation of the rate of stem radial variations

To assess the dynamics of stem radial variations, GAMs were fitted on stem radial size measurements for every year, every site, and each individual tree of each species. Fittings were then pooled together to represent the general dynamics of stem radial size variations by species, site, and year. The daily rate of stem radial variation was calculated as the daily differences in the stem radial variations predicted using GAMs.

Calculation of the daily rate of xylem size increase

The daily rate of xylem size increase was calculated from the rate of xylem cell production through cambial cell division, the radial diameter of the cambial cells, and the individual rates of cell diameter enlargement in the enlargement zone (Supplementary Fig. 1). First, we measured the radial diameter of cambial cells during the growing season using the measurement software Videomet^{TM} (Microvision instruments, France). We found values close to 7 µm for the different species, year, and sites (Supplementary Table 3). Therefore, we assumed that each cambial division leads to the formation of new cells of 7 µm in diameter. So, the daily rate of xylem size increase provided by the cambial zone (XSI_{CZ}, µm day^{-1}) is calculated simply by multiplying the rate of xylem cell production-(r_C, cell day^{-1}) by 7 µm cell^{-1}.

Moreover, the daily rate of xylem size increase provided by the enlargement zone (XSI_{EZ}, µm day^{-1}) was calculated as the sum of the individual rates of cell enlargement:

$$XSI_{EZ} = \sum_{i=1}^{n_E} r_{E,i}$$

where n_E is the daily number of cells in the enlargement zone, and $r_{E,i}$ is the enlargement rate ($\mu m\ day^{-1}$) of the cell i of the n_E cells.

The daily xylem size increase (XSI) was finally calculated as the sum of the contributions of xylem cell production-and enlargement:

$$XSI = XSI_{CZ} + XSI_{EZ}$$

Calculation of the daily rate of woody biomass production

The rates of xylem cell production and cellular differentiation were used to calculate the daily rate woody biomass production (Supplementary Fig. 1). First, a rate of primary wall deposition in the cambial zone was calculated from the rate of xylem cell production (r_C) through cambial cell division in the cambium and the thickness of the primary cell walls. For that, we measured the primary wall thickness during the growing season using Videomet™ (Microvision instruments, France) and found values close to 0.5 µm for the different species, year, and sites (Supplementary Table 3). Therefore, we assumed that each cambial division leads to the formation of a new cell with four primary walls of 0.5 µm in thickness: two in the tangential direction and with a span corresponding to the mean width of a radial file, as well as two in the radial direction and with a span equal to the radial diameter of a cambial cell (7 µm). The daily rate of primary wall formation in the dividing cells of the cambial zone ($r_{W,CZ}$, $\mu m^2\ day^{-1}$) is thus calculated as:

$$r_{W,CZ} = (r_C \times 2 \times 0.5\ \mu m \times RF_w) + (r_C \times 2 \times 0.5\ \mu m \times 7\ \mu m)$$

Similarly, we assumed that a given enlargement of a cell generates two primary walls of 0.5 µm in thickness and with a span corresponding to the lengthening of the cell. Therefore, the daily rate of radial primary wall formation in the enlarging cells of the enlargement zone ($r_{W,EZ}$, $\mu m^2\ day^{-1}$) was calculated from the daily xylem size increase provided by the

DOI: 10.1038/NPLANTS.2015.160

enlargement zone (XSI_{EZ}) as followed:

$$r_{W,EZ} = XSI_{EZ} \times 2 \times 0.5\ \mu m$$

Finally, the rate of wall-material deposition in the wall thickening zone ($r_{W,WZ}$, μm^2 day^{-1}) was calculated as the sum of the cellular rates of wall deposition.

$$r_{W,WZ} = \sum_{i=1}^{n_W} r_{W,i}$$

where n_W is the daily number of cells in the wall thickening zone, $r_{W,i}$ is the wall deposition rate (μm^2 day^{-1}) of the cell i of the n_W cells.

A sensitivity analysis was performed in order to assess the impact of the values of cambial cell diameter and primary wall thickness on the rate of woody biomass production; it showed that while the exact choice of these parameters slightly affects the absolute quantities of carbon, it has negligible impact on the intra-annual dynamics of woody carbon sequestration (Supplementary Figure 3).

The rate of wall deposition in the radial file was calculated as the sum of the rates of primary and secondary wall deposition. We estimated the number of radial files composing a tree ring at the periphery of the base of the stem by dividing the mean circumference at breast height of the studied trees the mean width of a radial file. After that, the total daily rate of wall deposition at the tree ring level ($r_{W,TR}$) was estimated as:

$$r_{w,TR} = r_{w,RF} \times n_{RF}$$

where n_{RF} is the estimated number of radial files composing a tree ring at the periphery at the base of the stem.

The total daily rate of wall deposition at the stem level ($r_{W,S}$) was obtained on the basis of a cone and from the height of the studied trees (H):

$$r_{W,S} = \frac{1}{3} \times H \times r_{W,TR}$$

Based on wall density of 1.5 g cm^{-3} (refs 20-22), and on a carbon percentage in wood of 50% of dry weight[23], we converted our daily volumetric wall deposition rate at the stem level to a daily rate of woody biomass production (WBP):

$$WBP = 1.5 \times r_{W,S} \times 0.5$$

This woody biomass production is expressed in gram of carbon per day (gC day^{-1}).

Proceeding this way, the rates of tangential primary wall deposition in the cambial zone, radial primary wall deposition in the enlargement zone, and wall deposition in the wall thickening zone were also separately extended at the tree stem level and converted into daily rates of biomass production. We thus obtained the daily rates of biomass production provided by the cambial zone, the enlargement zone, and the wall thickening zone, respectively. The relative contribution of these different carbon sinks on the woody biomass production could then be evaluated.

Using phenological observations of xylem tissue formation to estimate the timing of xylem size increase and woody carbon sequestration in northern hemisphere forest biomes

In addition to the detailed cellular-based quantifications described above and performed for the studied sites in northeast France, we built a global dataset of more widely available phenological observations of xylem tissue formation in order to estimate the timing of xylem size increase and woody biomass production in diverse coniferous forest biomes of the Northern Hemisphere. Xylem phenology data encompasses the beginning and the cessation of the periods of cell enlargement and cell-wall thickening during the year (Fig. 2). Usually, the beginning of the period of cell enlargement (b_E) is defined as the date at which 50% of the observed xylem cell radial files show at least one first enlarging cell; whereas the cessation of the period of cell enlargement (c_E) is defined as the date at which 50% of the

DOI: 10.1038/NPLANTS.2015.160

observed radial files show at most one last enlarging cell[14]. The beginning and the cessation of the period of cell-wall thickening (b_W and c_W) are computed following the same principles, but considering wall thickening cells.

On the one hand, the phenology of the cell enlargement period is very similar to the one of cell division[14], and these two processes drive xylem size increase. On the other hand, because the secondary walls form the bulk of biomass in trees[24], the wall thickening process drives the woody carbon sequestration. Consequently, we considered the phenology of the periods of cell enlargement and cell-wall thickening as proxies for the timing of xylem size increase and woody biomass production, respectively. The mean time-lag between xylem size increase and woody biomass production (L_m) was assessed from the differences observed in between the beginnings (b_E and b_W) and the cessations (c_W and c_E) of the periods of cell enlargement and cell-wall thickening (Fig. 2):

$$L_m = \frac{(b_W - b_E) + (c_W - c_E)}{2}.$$

The phenological data collected cover a broad geographical range, with 51 sites spread from 29.65°N to 67.50°N in latitude, -79.23°W to 100.18°E in longitude, and 15 to 3850 m ASL in altitude (Supplementary Table 1). Sites were classified in four different forest types (boreal, Mediterranean, subalpine, and temperate) according to their coordinates and altitudes.

Assessment of the phasing between the seasonal dynamics of xylem size increase, woody biomass production, and environmental factors

The materials and methods described above allowed us to draw a detailed picture of the intra-annual dynamics of xylem size increase and woody biomass production, in parallel to the seasonal course of environmental factors for each studied site, year and species in northeast France (Supplementary Figs 4, 5, 6). Cross-correlations were performed between these different time-series in order to assess the degree of synchronisation between the

seasonal dynamics of xylem size increase, woody biomass production, and the different environmental factors. Cross-correlation is a standard method for examining the relationship between two time series[25]. It is a measure of similarity of two series as a function of a time-lag applied to one of them. Therefore, the cross-correlation is helpful for identifying if two series are synchronised (*i.e.* the correlation between series is the highest with no time-lag) or not (*i.e.* the correlation increases when lagging one of the two series).

We further assessed dependency of xylem size increase and woody biomass production with the environmental factors using linear models. We focused on the time window when processes were active (between 5% and 95% of their realisation) in order to avoid zero values inflation. Within this time window, the intra-annual dynamics of a process was related to the seasonal course of climatic factors, after removing site and year effects in order to focus on seasonal variability.

References

1 Granier, A., Breda, N., Biron, P. & Villette, S. A lumped water balance model to evaluate duration and intensity of drought constraints in forest stands. *Ecol. Model.* **116**, 269-283 (1999).

2 Cuny, H. E. *et al.* Generalized additive models reveal the intrinsic complexity of wood formation dynamics. *J. Exp. Bot.* **64**, 1983-1994 (2013).

3 R: A language and environment for statistical computing. R Foundation for Statistical Computing, Vienna, Austria. ISBN 3-900051-07-0, URL http://www.R-project.org/. (2015).

DOI: 10.1038/NPLANTS.2015.160

4 Wood, S. N. *Generalized additive models: an introduction with R*. (Chapman and Hall/CRC, 2006).

5 Rossi, S., Anfodillo, T. & Menardi, R. Trephor: a new tool for sampling microcores from tree stems. *Iawa Journal* **27**, 89-97 (2006).

6 Forster, T., Schweingruber, F. H. & Denneler, B. Increment puncher: a tool for extracting small cores of wood and bark from living trees. *Iawa Journal* **21**, 169-180 (2000).

7 Deslauriers, A., Morin, H. & Begin, Y. Cellular phenology of annual ring formation of *Abies balsamea* in the Quebec boreal forest (Canada). *Can. J. For. Res.* **33**, 190-200 (2003).

8 Cosgrove, D. J. Expansive growth of plant cell walls. *Plant Physiol. Biochem.* **38**, 109-124 (2000).

9 Mellerowicz, E. J., Baucher, M., Sundberg, B. & Boerjan, W. Unravelling cell wall formation in the woody dicot stem. *Plant Mol. Biol.* **47**, 239-274, doi:10.1023/a:1010699919325 (2001).

10 Donaldson, L. A. Lignification and lignin topochemistry—an ultrastructural view. *Phytochemistry* **57**, 859-873 (2001).

11 Abe, H., Funada, R., Ohtani, J. & Fukazawa, K. Changes in the arrangement of cellulose microfibrils associated with the cessation of cell expansion in tracheids. *Trees-Struct. Funct.* **11**, 328-332 (1997).

12 Kutscha, N. P., Hyland, F. & Schwarzmann, J. M. Certain seasonal changes in balsam fir cambium and its derivatives. *Wood Sci. Technol.* **9**, 175-188 (1975).

13 Rossi, S., Deslauriers, A. & Morin, H. Application of the Gompertz equation for the study of xylem cell development. *Dendrochronologia* **21**, 33-39 (2003).

14 Rathgeber, C. B. K., Longuetaud, F., Mothe, F., Cuny, H. & Le Moguedec, G. Phenology of wood formation: Data processing, analysis and visualisation using R (package CAVIAR). *Dendrochronologia* **29**, 139-149 (2011).

15 Cuny, H. E., Rathgeber, C. B. K., Frank, D., Fonti, P. & Fournier, M. Kinetics of tracheid development explain conifer tree-ring structure. *New Phytol.*, doi:10.1111/nph.12871 (2014).

16 Hastie, T. & Tibshirani, R. Generalized additive models. *Statistical Science* **1**, 297-318 (1986).

17 McCullagh, P. & Nelder, J. A. *Generalized Linear Models*. (Chapman and Hall, 1983).

18 Zuur, A. F., Ieno, E. N., Walker, N. J., Saveliev, A. A. & Smith, G. M. *Mixed effects models and extensions in ecology with R*. (Springer-Verlag, 2009).

DOI: 10.1038/NPLANTS.2015.160

19 Yee, T. W. & Mitchell, N. D. Generalized additive models in plant ecology. *J. Veg. Sci.* **2**, 587-602, doi:10.2307/3236170 (1991).

20 Zauer, M., Pfriem, A. & Wagenführ, A. Toward improved understanding of the cell-wall density and porosity of wood determined by gas pycnometry. *Wood Sci. Technol.* **47**, 1197-1211 (2013).

21 Plötze, M. & Niemz, P. Porosity and pore size distribution of different wood types as determined by mercury intrusion porosimetry. *Eur. J. Wood Wood Prod.* **69**, 649-657 (2011).

22 Pfriem, A., Zauer, M. & Wagenführ, A. Alteration of the pore structure of spruce (Picea abies (L.) Karst.) and maple (Acer pseudoplatanus L.) due to thermal treatment as determined by helium pycnometry and mercury intrusion porosimetry. *Holzforschung* **63**, 94-98 (2009).

23 Lamlom, S. & Savidge, R. A reassessment of carbon content in wood: variation within and between 41 North American species. *Biomass Bioenergy* **25**, 381-388 (2003).

24 Zhong, R. & Zheng-Hua, Y. Secondary cell walls. *Encyclopedia of Life Sciences* (2009).

25 Chatfield, C. *The analysis of time series: an introduction*. 6 edn, (Chapman & Hall/CRC Press, 2003).

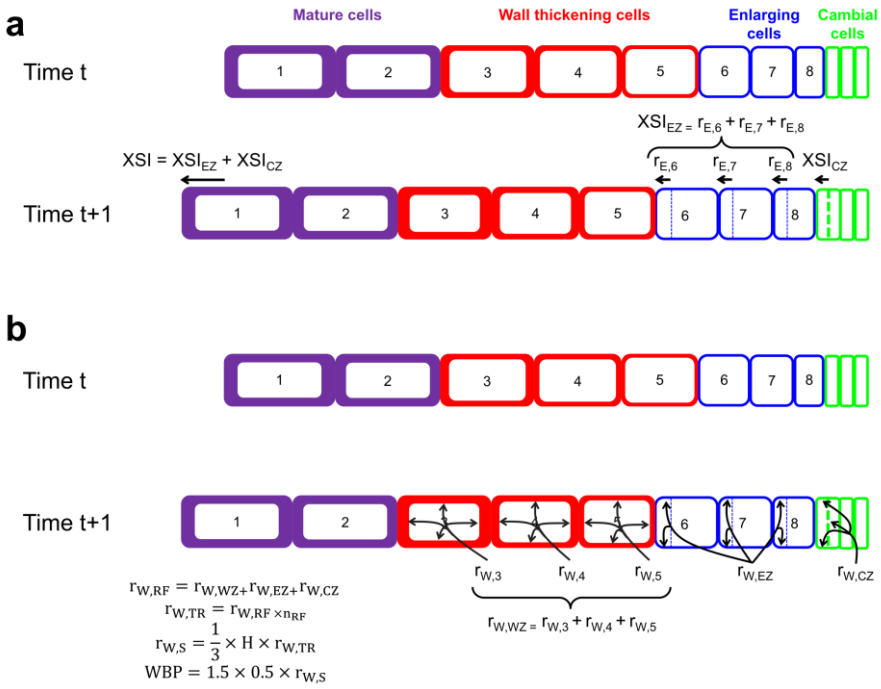

Supplementary Figure 1. Computation of the daily rates of xylem size increase and woody biomass production. a, Computation of the daily xylem size increase (XSI), which integrates the contributions of the cell enlargement (XSI_{EZ}) and of the cambial zones (XSI_{CZ}). XSI_{EZ} is computed from the individual rates of cellular enlargement ($r_{E,i}$) of the i^{th} enlarging cells, whereas XSI_{CZ} is computed from the rate of xylem cell production (Supplementary Methods). **b**, Computation of the daily woody biomass production (WBP). The rate of wall deposition in the cell radial file ($r_{W,RF}$) integrates the contributions of the wall thickening ($r_{W,WZ}$), enlargement ($r_{W,EZ}$) and cambial zones ($r_{W,CZ}$). $r_{W,WZ}$ is computed as the sum of the individual rates of wall deposition ($r_{W,i}$) of the i^{th} thickening cells, whereas $r_{W,EZ}$ and $r_{W,CZ}$ are computed from XSI_{EZ} and the rate of xylem cell production, respectively (Supplementary Methods). The total daily rate of wall deposition at the tree ring level ($r_{W,TR}$) is calculated from $r_{W,RF}$ after estimating the total number of radial files (n_{RF}) in the ring. Then, $r_{W,TR}$ is used to calculate the daily rate of wall deposition at the stem level ($r_{W,S}$) from the height of the studied trees (H) and on the basis of a cone. Finally, the daily woody biomass production (WBP) is computed from $r_{W,S}$ based on an apparent density of the wall of 1.5 g cm^{-3} and on a carbon percentage in wood being 50% of dry weight.

DOI: 10.1038/NPLANTS.2015.160

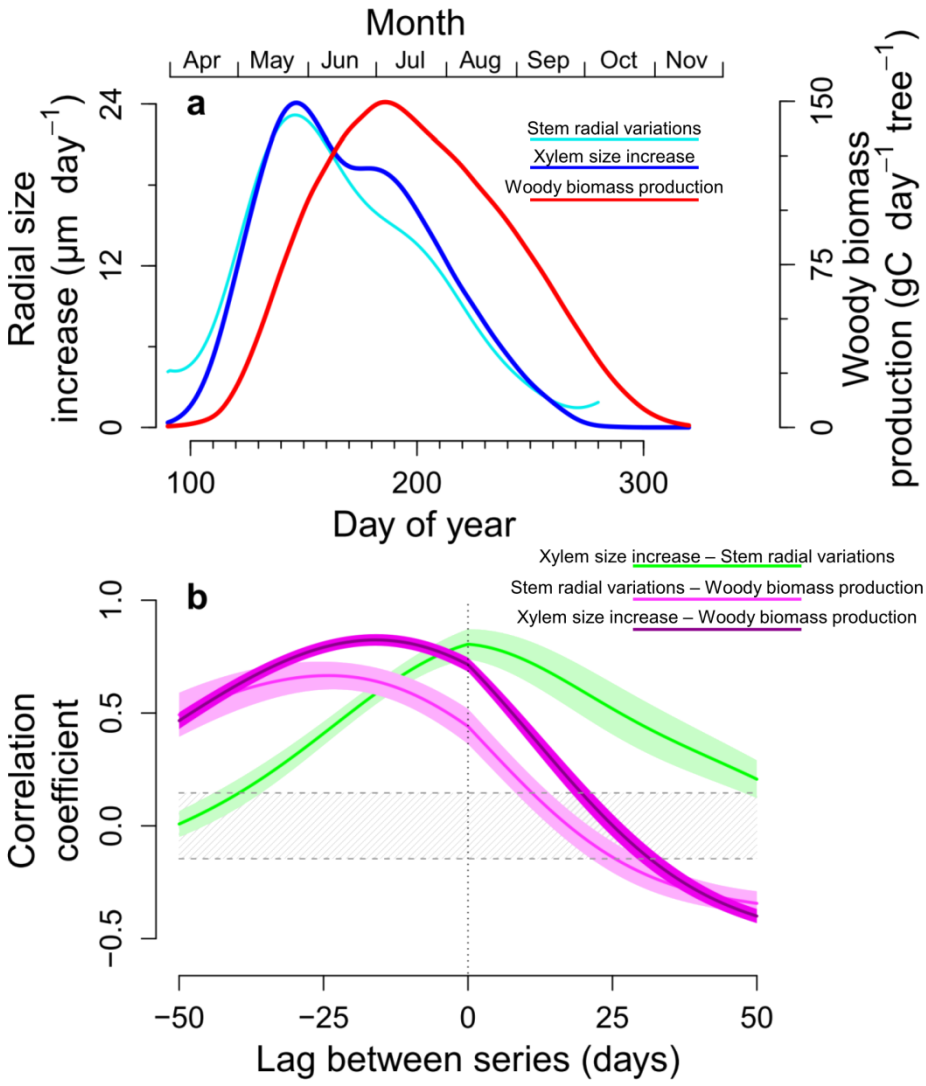

Supplementary Figure 2. Comparison of the seasonal dynamics of external stem radial variations, xylem size increase, and woody biomass production. **a**, Seasonal dynamics of stem radial variations, xylem size increase, and woody biomass production. **b**, Cross-correlations between the seasonal dynamics of stem radial variations, xylem size increase, and woody biomass production. In **a**, the different curves represents the means for the three northeast France sites (Vosges mountains), with the three species (Norway spruce, Scots pine and silver fir) monitored during three years (2007-2009). In **b**, the different curves indicate the mean correlation coefficients for northeast France (over sites, species and years), shaded area around lines represents 95% confidence interval around mean, and hatched area represents coefficient values above significance level ($P > 0.05$).

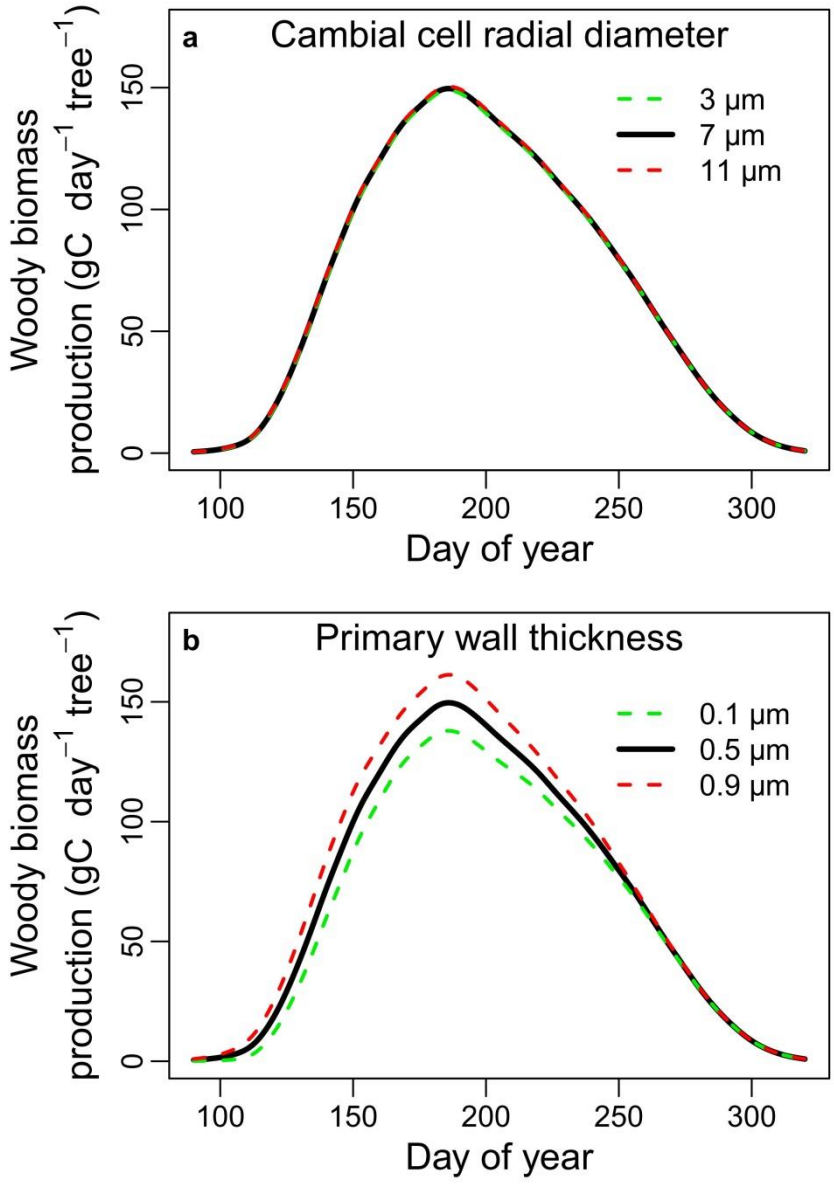

Supplementary Figure 3: Sensitivity analysis of the computation of the rate of woody biomass production. a, Variation of the rate of woody biomass production according to the value of the cambial cell radial diameter. **b**, Variation of the rate of woody biomass production according to the value of the primary wall thickness. Data are means for the three northeast France sites (Vosges mountains), with the three species (silver fir, Norway spruce and Scots pine) monitored during three years (2007-2009). Note that the ranges of variation apply for the two parameters are far beyond the variability observed on the measurements performed on the anatomical sections (see Supplementary Table 3).

DOI: 10.1038/NPLANTS.2015.160

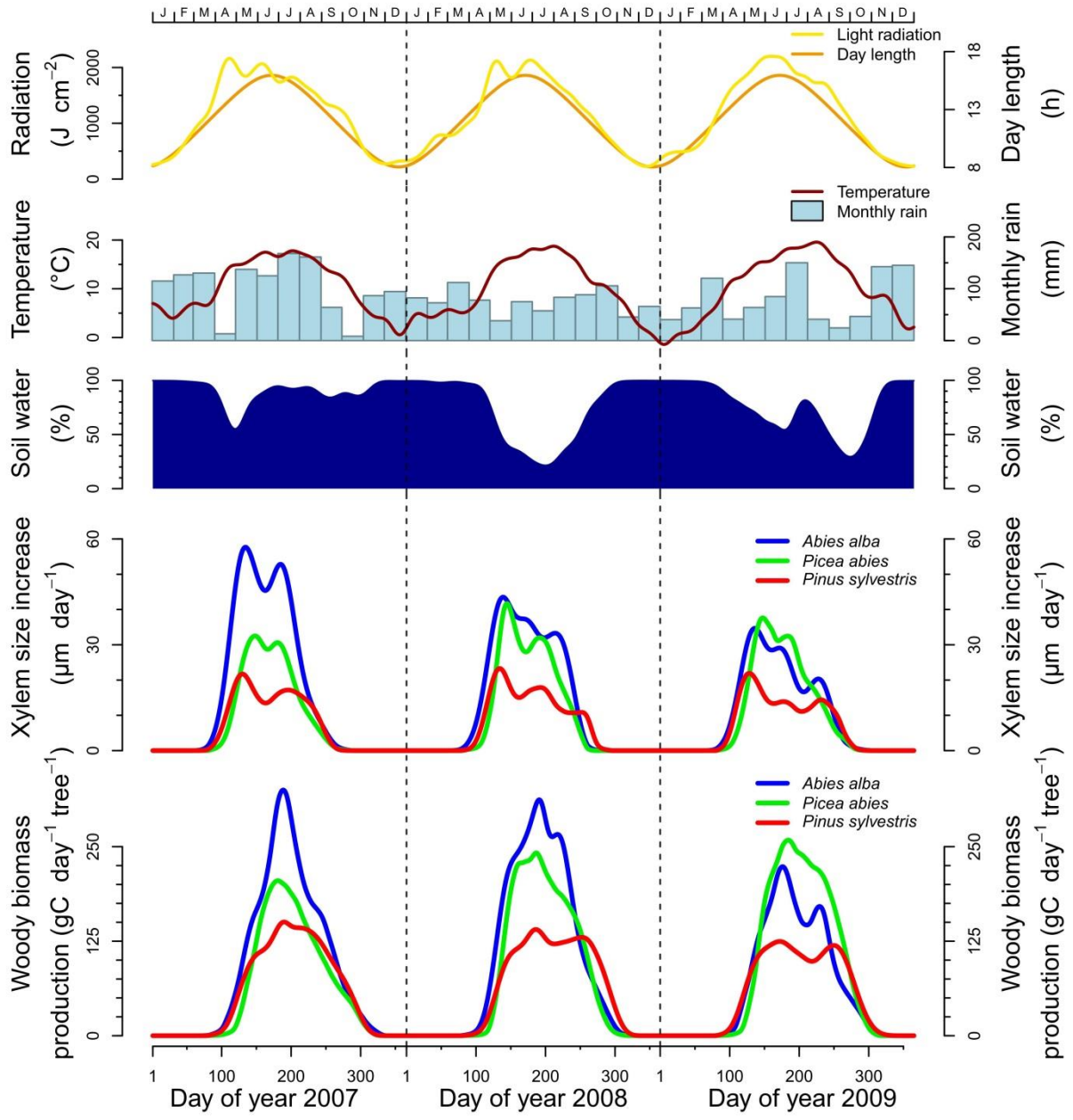

Supplementary Figure 4. Seasonal evolution of environmental factors, xylem size increase and woody biomass production for the three years of monitoring at Walscheid site in northeast France. Upper x-axis indicates the months. For xylem size increase and woody biomass production, each line represents the mean of 5 trees for one species.

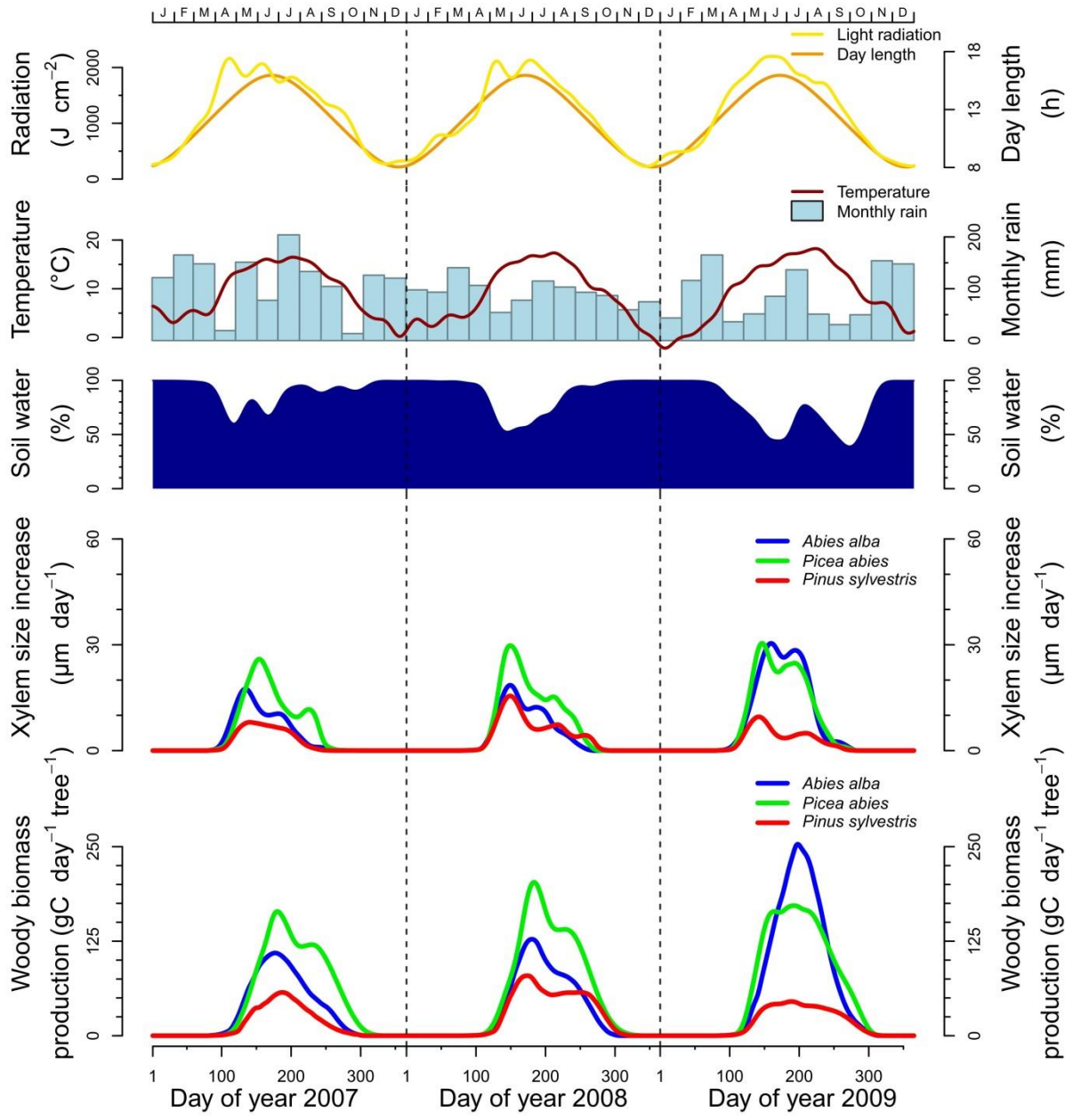

Supplementary Figure 5. Seasonal evolution of environmental factors, xylem size increase and woody biomass production for the three years of monitoring at Abreschviller site in northeast France. Upper x-axis indicates the months. For xylem size increase and woody biomass production, each line represents the mean of 5 trees for one species.

DOI: 10.1038/NPLANTS.2015.160

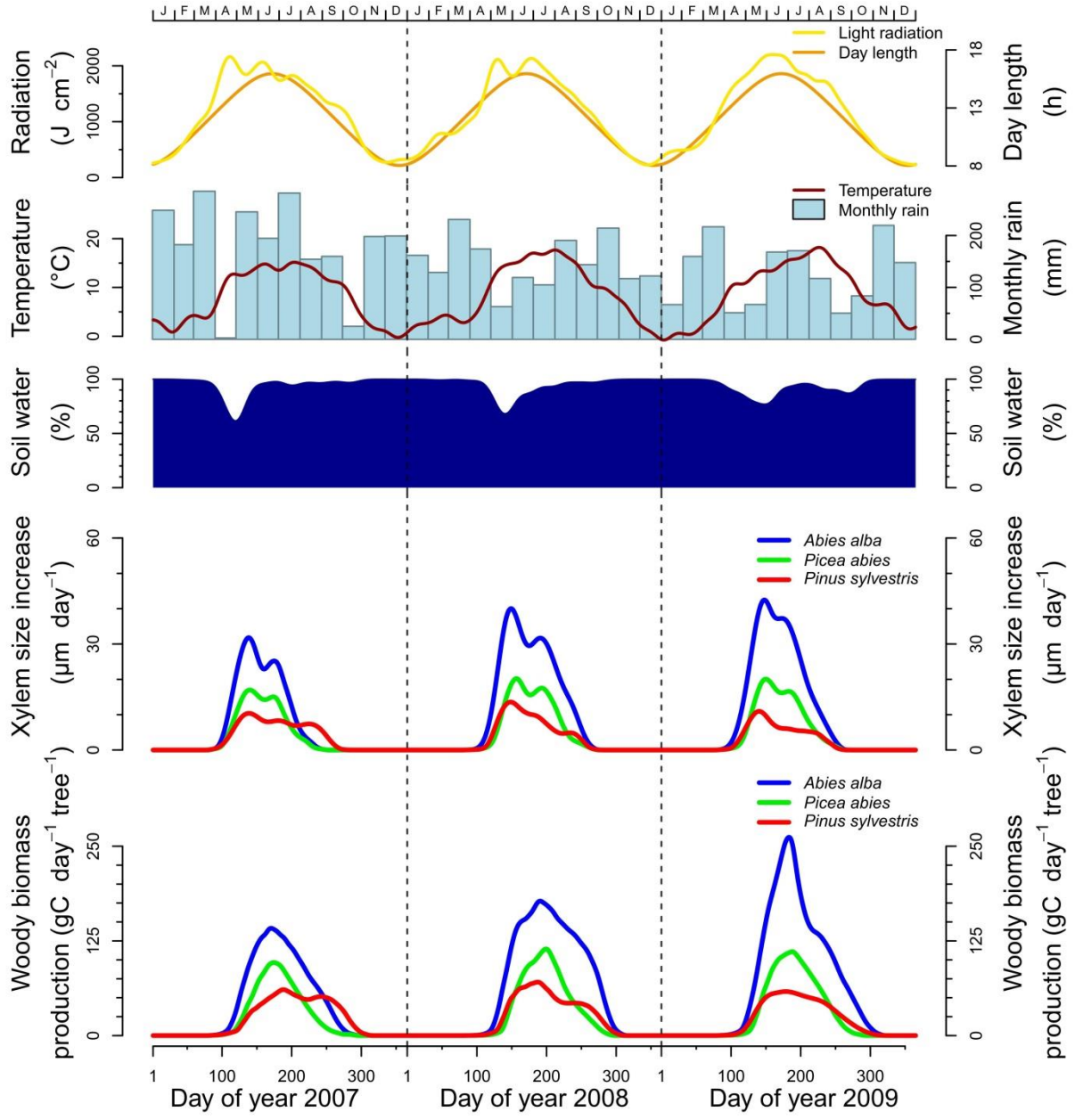

Supplementary Figure 6. Seasonal evolution of environmental factors, xylem size increase and woody biomass production for the three years of monitoring at Grandfontaine site in northeast France. Upper x-axis indicates the months. For xylem size increase and woody biomass production, each line represents the mean of 5 trees for one species.

Supplementary Table 1: site locations, studied species, monitored years, and number of sampled trees in the Northern Hemisphere dataset on wood formation phenology.

Biome	Country	Site	Latitude (°N)	Longitude (-°W. +°E)	Altitude (m ASL)	Species	Years monitored	Number of trees
Boreal	Canada	Angliers	47.54	-79.23	283	*Picea mariana*	2005 to 2006	5
		Arvida	48.43	-71.15	80	*Abies balsamea*	1999 to 2000	18
		Bernatchez	48.85	-70.33	611	*Picea mariana*	2002 to 2010	5 to 10
		Chicobi	49.28	-78.32	324	*Picea mariana*	2005 to 2006	5
		Camp Daniel	50.68	-72.18	487	*Picea mariana*	2002 to 2010	5 to 10
		Mistassibi	49.71	-71.93	342	*Picea mariana*	2002 to 2010	5 to 10
		Muskuchii	49.95	-78.72	271	*Picea mariana*	2005 to 2006	5
		Simoncouche	48.21	-71.25	338	*Abies balsamea*	2005 to 2008	10
						Picea mariana	2002 to 2010	5 to 10
	Finland	Hyytiälä	61.90	24.30	181	*Pinus sylvestris*	2008 to 2010	4 to 5
						Picea abies	2008 to 2010	4
		Kivalo	66.20	26.40	140	*Picea abies*	2009	5
						Pinus sylvestris	2008	5
		Ruotsinkylä	60.20	25.00	60	*Pinus sylvestris*	2008 to 2010	4
						Picea abies	2008 to 2010	4
		Solböle	60.00	23.00	30	*Picea abies*	2008	4
		Värriö	67.50	29.40	390	*Pinus sylvestris*	2008 to 2009	4
	Russia	Hilltop	64.30	100.18	589	*Larix gmelinii*	2011 to 2012	4 to 5
		Riverbank	64.30	100.18	140	*Larix gmelinii*	2011 to 2012	4 to 5
Mediterranean	Portugal	Tocha	40.35	-8.82	15	*Pinus pinaster*	2010 to 2011	8
	Spain	Guardamar	38.10	-0.65	15	*Pinus halepensis*	2005	12
		Jarafuel	39.16	-1.15	850	*Pinus halepensis*	2004	6
		Maigmo	38.52	-0.64	845	*Pinus halepensis*	2004 and 2005	6
		Moncayo High	41.80	-1.82	1600	*Pinus sylvestris*	2011 to 2013	6
		Moncayo Low	41.80	-1.82	1200	*Pinus sylvestris*	2011 to 2013	6
		Peñaflor	41.78	-0.72	340	*Juniperus thurifera*	2006 and 2010	10
						Pinus halepensis	2006 and 2010	10
		Torrijas	39.99	-0.91	1600	*Pinus sylvestris*	2005	5
		Villarroya de los Pinares	40.50	-0.62	1690	*Pinus sylvestris*	2005	5
Subalpine	Austria	Patscherkofel timberline	47.20	11.45	1950	*Pinus cembra*	2007	6
		Patscherkofel treeline	47.20	11.45	2110	*Pinus cembra*	2007	6
	China	Sygera Mountains	29.65	94.71	3850	*Abies georgei*	2007 to 2008	5
	Italy	Pollino	39.90	16.20	2053	*Pinus leucodermis*	2003 to 2004	10
						Larix decidua	2001 to 2005	10
		Timber line 5T1	46.45	12.13	2085	*Picea abies*	2001 to 2005	10
						Pinus cembra	2001 to 2005	10
		Tree line 5T2	46.45	12.13	2156	*Larix decidua*	2002 to 2005	5
						Picea abies	2002 to 2005	1
						Pinus cembra	2002 to 2005	5
		Val di Susa	45.05	6.66	2030	*Larix decidua*	2003 to 2004	5
						Pinus cembra	2003 to 2004	5
						Pinus uncinata	2003 to 2004	5
	Switzerland	Lotschental N19	46.38	7.75	1900	*Larix decidua*	2007 to 2008	4
						Picea abies	2007 to 2008	4
		Lotschental N22	46.38	7.75	2150	*Larix decidua*	2007 to 2008	4
		Lotschental S19	46.38	7.75	1900	*Larix decidua*	2007 to 2008	4
						Picea abies	2007 to 2008	4
		Lotschental S22	46.38	7.75	2150	*Larix decidua*	2007 to 2008	4
Temperate	Austria	Tschirgant xeric	47.23	10.85	750	*Pinus sylvestris*	2007 to 2010	6 to 8
		Tschirgant dry-mesic	47.23	10.85	750	*Pinus sylvestris*	2007 to 2010	5 to 8
	Czech Republic	Lucni hora 1	50.71	15.66	1310	*Picea abies*	2010 to 2012	6 to 9
		Lucni hora 2	50.72	15.67	1450	*Picea abies*	2010 to 2012	6 to 9
		Rajec-Nemice	49.44	16.69	620	*Picea abies*	2009 to 2011	6
	France	Abreschviller	48.48	7.15	430	*Abies alba*	2007 to 2009	5
						Picea abies	2007 to 2009	5
						Pinus sylvestris	2007 to 2009	5
		Amance	48.75	6.33	270	*Abies alba*	2006 to 2008	5
						Pinus sylvestris	2006 to 2008	5
		Grandfontaine	48.60	7.13	643	*Abies alba*	2007 to 2009	5
						Picea abies	2007 to 2009	5
						Pinus sylvestris	2007 to 2009	5
		Walscheid	48.63	7.15	370	*Abies alba*	2007 to 2009	5
						Picea abies	2007 to 2009	5
						Pinus sylvestris	2007 to 2009	5
	Slovenia	Menina planina	46.27	14.75	1200	*Picea abies*	2009 to 2011	5 to 10
		Panska reka	46.00	14.66	400	*Picea abies*	2009 to 2011	6
	Switzerland	Lotschental N08	46.38	7.75	800	*Larix decidua*	2008	4
						Picea abies	2008	4
		Lotschental N13	46.38	7.75	1350	*Larix decidua*	2007 to 2008	4
						Picea abies	2007 to 2008	4
		Lotschental N16	46.38	7.75	1600	*Larix decidua*	2007 to 2008	4
						Picea abies	2007 to 2008	4
		Lotschental S16	46.38	7.75	1600	*Larix decidua*	2007 to 2008	4
						Picea abies	2007 to 2008	4

DOI: 10.1038/NPLANTS.2015.160

Supplementary Table 2: Main characteristics (mean ± SE) of the monitored trees from the three studied species (silver fir, Norway spruce and Scots pine) in three temperate forests in northeast France, including age, diameter at breast height (DBH), height (H), and projected crown area (CA).

Site	Species	Age (Yr)	DBH (cm)	H (m)	CA (m²)
Walscheid	*Abies alba*	94 ± 2	56 ± 1	31 ± 1	43 ± 5
	Picea abies	89 ± 4	53 ± 2	32 ± 1	40 ± 5
	Pinus sylvestris	95 ± 3	52 ± 3	31 ± 1	41 ± 10
Abreschviller	*Abies alba*	135 ± 2	60 ± 3	36 ± 1	28 ± 5
	Picea abies	85 ± 7	41 ± 2	32 ± 1	16 ± 2
	Pinus sylvestris	162 ± 3	33 ± 3	36 ± 1	20 ± 5
Grandfontaine	*Abies alba*	73 ± 3	57 ± 3	31 ± 1	37 ± 6
	Picea abies	74 ± 4	55 ± 4	33 ± 1	30 ± 7
	Pinus sylvestris	119 ± 3	53 ± 2	27 ± 1	29 ± 2
Means	*Abies alba*	101 ± 6	58 ± 2	33 ± 1	36 ± 3
	Picea abies	83 ± 3	49 ± 2	32 ± 1	29 ± 4
	Pinus sylvestris	126 ± 8	56 ± 2	32 ± 1	30 ± 4

Supplementary Table 3: Values (means ± standard deviation) of cambial cell radial diameter and primary wall thickness during the growing season for the different sites, years, and species in northeast France. Measurements were performed during the growing season for one tree per site, year, and species, with approximately 40 measurements for each variable on each sample.

Site	Year	Species	Cambial cell radial diameter	Primary wall thickness
Walscheid	2007	*Abies alba*	6.7 ± 2.4	0.48 ± 0.12
		Picea abies	6.7 ± 1.7	0.50 ± 0.14
		Pinus sylvestris	7.0 ± 2.1	0.50 ± 0.08
	2008	*Abies alba*	7.8 ± 2.6	0.56 ± 0.07
		Picea abies	7.0 ± 3.9	0.50 ± 0.07
		Pinus sylvestris	6.6 ± 4.0	0.51 ± 0.08
	2009	*Abies alba*	7.0 ± 3.2	0.53 ± 0.08
		Picea abies	6.7 ± 3.3	0.51 ± 0.10
		Pinus sylvestris	7.1 ± 3.6	0.49 ± 0.07
Abreschviller	2007	*Abies alba*	7.3 ± 2.2	0.49 ± 0.10
		Picea abies	6.8 ± 2.8	0.50 ± 0.14
		Pinus sylvestris	6.8 ± 2.6	0.56 ± 0.11
	2008	*Abies alba*	6.9 ± 3.0	0.46 ± 0.10
		Picea abies	6.9 ± 3.0	0.48 ± 0.07
		Pinus sylvestris	7.0 ± 2.3	0.48 ± 0.10
	2009	*Abies alba*	7.0 ± 2.9	0.52 ± 0.07
		Picea abies	7.0 ± 3.0	0.46 ± 0.08
		Pinus sylvestris	7.3 ± 3.5	0.48 ± 0.08
Grandfontaine	2007	*Abies alba*	6.9 ± 2.3	0.49 ± 0.11
		Picea abies	6.9 ± 2.6	0.47 ± 0.09
		Pinus sylvestris	7.0 ± 2.4	0.48 ± 0.09
	2008	*Abies alba*	6.8 ± 2.4	0.54 ± 0.08
		Picea abies	6.8 ± 2.2	0.58 ± 0.10
		Pinus sylvestris	7.1 ± 2.8	0.50 ± 0.08
	2009	*Abies alba*	7.2 ± 2.2	0.50 ± 0.13
		Picea abies	6.9 ± 3.6	0.52 ± 0.14
		Pinus sylvestris	6.9 ± 2.8	0.52 ± 0.06
Means			7.0 ± 2.8	0.51 ± 0.09